SF 298 MASTER COPY KEEP THIS COPY FOR REPRODUCTION PURPOSES

REPORT DOCUMENTATION PAGE

Form Approved
OMB NO. 0704-0188

1. AGENCY USE ONLY *(Leave blank)*	2. REPORT DATE	3. REPORT TYPE AND DATES COVERED
	February 1996	Final 1 Dec 94 - 28 Feb 96

4. TITLE AND SUBTITLE

Instrument for Damage Evaluation/Characterization of Steel Belted Radial Tires

5. FUNDING NUMBERS

DAAL04-95-1-0012

6. AUTHOR(S)

Henrique L. M. dos Reis and Paul J. Golko

7. PERFORMING ORGANIZATION NAMES(S) AND ADDRESS(ES)

Department of General Engineering
University of Illinois at Urbana-Champaign
104 S. Mathews
Urbana, Illinois 61801

8. PERFORMING ORGANIZATION REPORT NUMBER

9. SPONSORING / MONITORING AGENCY NAME(S) AND ADDRESS(ES)

U.S. Army Research Office
P.O. Box 12211
Research Triangle Park, NC 27709-2211

10. SPONSORING / MONITORING AGENCY REPORT NUMBER

ARO 33646.1-MS-RIP

11. SUPPLEMENTARY NOTES

The views, opinions and/or findings contained in this report are those of the author(s) and should not be construed as an official Department of the Army position, policy or decision, unless so designated by other documentation.

12a. DISTRIBUTION / AVAILABILITY STATEMENT

Approved for public release; distribution unlimited.

12 b. DISTRIBUTION CODE

13. ABSTRACT *(Maximum 200 words)*

A prototype instrument capable of detecting/evaluating ply cord fatigue damage, i.e., the zipper mode of failure, in radial steel-belted truck tires has been developed. The instrument is production-oriented and capable of being used for on-line inspection of new or retreaded tires. Furthermore, the instrument is also capable of providing color-coded scans, thereby reducing the possibility of operator error which could result in damaged tires being placed in service.

14. SUBJECT TERMS

Acousto-ultrasonics, Zipper, Radial Truck Tires, Ply Cords, Fatigue Damage, Nondestructive Evaluation, Ultrasonics

15. NUMBER IF PAGES
33

16. PRICE CODE

17. SECURITY CLASSIFICATION OR REPORT	18. SECURITY CLASSIFICATION OF THIS PAGE	19. SECURITY CLASSIFICATION OF ABSTRACT	20. LIMITATION OF ABSTRACT
UNCLASSIFIED	UNCLASSIFIED	UNCLASSIFIED	UL

Instrument for Damage Evaluation/Characterization of Steel Belted Radial Tires

FINAL PROGRESS REPORT

Henrique L. M. dos Reis
Paul J. Golko

February, 1996

U.S. ARMY RESEARCH OFFICE

CONTRACT NUMBER: DAAH04-95-1-0012

University of Illinois at Urbana-Champaign
Urbana, Illinois

ABSTRACT

A prototype instrument capable of detecting/evaluating ply cord fatigue damage, i.e., the zipper mode of failure, in radial steel-belted truck tires has been developed. The instrument is production-oriented and capable of being used for on-line inspection of new or retreaded tires. Furthermore, the instrument is also capable of providing color-coded scans, thereby reducing the possibility of operator error which could result in damaged tires being placed in service.

KEYWORDS: Acousto-ultrasonics, Zipper, Radial Truck Tires, Ply Cords, Fatigue Damage, Nondestructive Evaluation, Ultrasonics.

TABLE OF CONTENTS

LIST OF FIGURES

INTRODUCTION

It has been estimated that by the year 2000, twice as many retreaded truck tires as new tires would be sold in the United States [1]. The use of retreaded tires can result in significant financial and environmental savings. In order for these savings to materialize, however, it is essential that used tire casings do not fail in service during the projected life of a retread. Therefore, used tires must be inspected prior to retreading to evaluate the structural integrity of the casings and determine their suitability for further use.

Underinflated (80% or less than recommended operating cold inflation pressures or runflat) radial truck tires can be subjected to steel cord fatigue damage in the upper sidewall area caused by overflexing of the tire. When the tire is being serviced, often during the retreading or the remounting and inflation steps, weakened cords may break with rupture of the upper side wall (this failure mode is usually called the *Zipper Failure Mode*) with potential catastrophic consequences such as loss of life.

Clearly, the inspection of all tire casings prior to retreading for this and other types of damage would be desirable. Some nondestructive testing devices, such as the ones based upon radioscopy, may show (but not always) this hazard condition if the cords are already broken. However, this approach is expensive and if the cords are not yet broken radioscopy does not evaluate the residual strength of the tire side walls creating a very serious safety hazard condition. Therefore, a new, inexpensive, rapid, and reliable method for detecting damage in radial ply cords is needed.

In a study performed at the University of Illinois at Urbana-Champaign, Acousto-Ultrasonics (AU) was used to detect ply cord damage in steel belted radial truck tires [2-5]. In the AU technique, an ultrasonic pulse is injected into the material being examined by one transducer and, after traveling through the material, is received by another transducer. The characteristics of the waveforms arriving at the receiving transducer are determined by the condition of the material through which the ultrasonic waves propagate. To quantify these characteristics, the AU waveform data is analyzed using the stress-wave-factor (SWF) approach. Although the stress-wave-factor does not have a standard definition, it is regarded to be any waveform parameter in any domain, such as the time or frequency, which helps in characterizing the material being inspected. In this study, several SWF's were used to detect radial cord damage, including the energy and rectified area in the time domain, as well as the maximum amplitude, frequency of maximum amplitude, and area in the frequency domain. In references [6-7] the reader can find in detail all the stress wave factors used in this study. As shown in References [2-5], these SWF's were successfully correlated with the severity and types of damage found in a new tire with seeded defects

and in tires with cord fatigue damage resulting from field use and flywheel testing.

The SWF has already been correlated with the mechanical strength of composite materials by Vary and Lark [8], Williams and Lampert [9], Kautz [10], and Govada, et al. [11]. SWF measurements have also been correlated, by the author of this study, with damage in wire rope [12], with swelling of wood products [13], with the adhesive bond strength between rubber and steel [14], and with the adhesive bond strength of connections in wood structures [15,16]. A good review of analytical ultrasonics in materials research and testing is given in references [17-19].

The main goal of this project is to extend on the work of the above study by developing a semi-automated acousto-ultrasonic prototype tire inspection machine. Once a tire is secured in the machine, the acousto-ultrasonic data would be collected, analyzed, and interpreted automatically using a computer. The results of the inspection would indicate the type and extent of damage found in the region where zipper failures normally occur. Based on the results of the inspection, a decision could be made whether the tire should be accepted for retreading as is, repaired and then retreaded, or scrapped due to insufficient structural integrity of the casing. The development of this prototype is a significant step toward the goal of inspecting all tire casings prior to retreading using this technology.

The work completed up to date, including hardware and software development as well as preliminary testing results, are presented within this report. Recommendations for future work are also outlined.

PROTOTYPE DESCRIPTION

The prototype acousto-ultrasonic tire inspection machine constructed up to date consists of several groups of components; namely, the base machine, transducer fixture, data acquisition system, and computer software.

The base machine is a modified version of the INSTA-SPECT Inspection/Repair Station purchased from ATEC, Inc., a photograph of which is shown in Figure 1(a) with a tire in a mounted position. The internal components are shown in more detail in Figure 1(b). In its original form, this machine is used in industry for manual tire inspection and repair. The main features of the machine are the ramp, which facilitates tire placement onto the machine, the rollers, which rotate the tire during inspection, the spreader arms, which pull the sidewalls of the tire apart to enhance visibility of inner surfaces, and the compressed air motor and associated drivetrain, which drive the rollers.

Several modifications and additions have been made to the original machine to convert it for acousto-ultrasonic tire inspection. First, the original air motor and gearbox were replaced by an electric stepper motor (Superior Electric model MH172-FD8030) and a matching 10:1 precision gearbox (Bayside, Inc. model NE 56) so that tire rotation/orientation can be controlled. Second, the original chain drive system was replaced by timing belts and sprockets in order to minimize backlash and thus increase angular positioning accuracy. Third, two sets of fixed support rollers were added, one on each side of the tire, to improve tire guidance and axial positioning consistency.

The motor control system is shown schematically in Figure 2. It consists of the stepper motor mentioned above, a Superior Electric model SS2000D12 stepper motor drive, a LC-DSP Motion Controller board from Motion Engineering, Inc., a Dell Computer Corporation 486 computer, and a manual switch. Motor motion is achieved by executing computer commands which are translated by the LC-DSP board and the drive into a series of electrical pulses which in turn energize the motor. The manual switch serves to stop the motor in an emergency by cutting off power to the motor drive.

Two ultrasonic transducers from Quality Materials Inspection (QMI), Inc., (model RP-100) shown in Figure 3 together with a cross section of a tire, were selected for acousto-ultrasonic measurements. A special fixture was designed and constructed to attach the transducers to the machine which would allow for testing of tires of various sizes and geometries. A photograph of the fixture as it appears mounted on the machine with the transducers in contact with the tire is shown in Figure 4. The fixture is manually adjusted to position the transducers normal to the tire outer sidewall surface and radially along the cords, and to align the transducer roller axes with the center of the tire. It provides contact

pressure between the transducers and the tire directed along the transducer axes while the tire is in motion. Due to the complicated tire geometry alone, as well as compliance considerations resulting from irregularities in tire geometry, the fixture has a total of twelve degrees of freedom.

The data acquisition system of the prototype machine is shown schematically in Figure 5. It consists of the two ultrasonic transducers, a Panametrics model 5055PRM Pulser/Receiver, a Krohn-Hite Corporation model 3988 Low-Pass/High-Pass Butterworth/Bessel Dual Channel Filter, a Sonix STR*8100D analog-to-digital (A/D) converter board, and the computer described previously. During preliminary testing, the pulser/receiver was pulsed at 500 pulses/second at the highest energy setting (level 4), the attenuation was set at 40 dB, and the gain was 60 dB. The preamplifier gain was approximately 52 dB and the built-in filter had a bandpass between 25 kHz and 25 MHz. The Krohn-Hite filter was operated in bandpass mode between the frequencies of 80 kHz and 500 kHz. The sampling frequency of the A/D board was 1.5625 MHz and the sampling duration was 327 ms.

The software component of the prototype machine is a menu-driven computer program written in the C language consisting of several integrated modules: data collection, analysis, results, and graphics. The data collection module incorporates the control of tire motion and collection of ultrasonic waveforms. This module allows for one of two methods to be employed in automatic tire scanning. In the first method, the tire is rotated through a predetermined angular interval intermittently and data is collected while the tire is not in motion. In the second method, the tire is rotated continuously and data is collected at fixed angular locations while the tire is in motion. The first method was used for preliminary testing in order to duplicate the conditions used in previous work. However, the second method is preferable since it is generally faster than the first and eliminates the vibrations associated with intermittent motion of the tire. Consequently, the continuous scanning method has been used in most of the early testing completed up to date. The data collected using this module is stored in a file on the computer hard disk.

The analysis module is used to compute various stress-wave-factors for each of the collected acousto-ultrasonic waveforms. Presently, a total of thirty-two SWF's are calculated for both the full waveform and a selected time partition of the waveform. Among these are the rectified area, energy, peak amplitude, and threshold crossings in the time domain, and the area, energy, maximum amplitude, and frequency of maximum amplitude in the frequency domain.

The results module allows for display of scan results in several forms. The user can choose to view the time domain representation of the individual waveforms along with

the corresponding magnitude of the Fast Fourier Transform of the signal, plots of SWF's versus location on the tire, or SWF results in the form of color-coded two-dimensional tires, with different colors assigned to different ranges of SWF values.

The graphics module supplements the above modules by providing menus and other graphics on the monitor. It also permits color and black-and-white hardcopy output of the results to be generated.

PROTOTYPE SAMPLE RESULTS

Several tires with radial cord damage sustained in the field have been examined using the prototype tire inspection machine with the ultrasonic roller transducers. Some preliminary results are presented in this section for one side of a tire containing significant field damage that was obtained from the American Retreaders Association.

In examining this tire, the pertinent ultrasonic equipment settings were maintained as described previously. The transmitting and receiving transducers were placed approximately 0.9 inches and 0.3 inches from the edges of the scuff rib, respectively, the transmitting transducer being closer to the center of the tire, for a total center-to-center transducer separation distance of approximately 2.0 inches as shown in Figure 3. The tire was scanned in the continuous mode (that is, data was collected while the tire was in motion) with ultrasonic measurements recorded every 0.3 degrees of tire rotation, for a total of 1200 sample locations. This angular sampling interval was chosen since it is slightly smaller than the spacing between radial cords on the tire at the transducer locations.

A typical waveform and the corresponding frequency spectrum collected from an undamaged region in the tire is shown in Figure 6. The angular location on the tire where this sample was obtained was 182.1 degrees from the startpoint. A typical waveform and frequency spectrum obtained from a region in the tire containing ply cord fatigue damage is shown in Figure 7. The location of this sample was 239.6 degrees from the startpoint.

Various stress-wave-factors were computed for each sample location for the full time domain record as well as a time partition of the waveform. Figures 8 and 9 are plots of energy versus position on the tire for the entire waveforms and 17.9 ms partition of the waveforms, starting at 26.9 ms and ending at 44.8 ms, respectively. Plots of the peak amplitude of the entire and partitioned waveforms are shown in Figures 10 and 11, respectively. In addition, plots of the area SWF in the frequency domain for the full and partitioned waveforms are also shown in Figures 12 and 13, respectively.

The stress-wave-factor results can also be presented in the form of color-coded two-dimensional tire diagrams, where different colors are assigned to various ranges of SWF values. Using a gray scale, Figures 14 through 19 show the same SWF's in this form as those of Figures 8 through 13, in the same order. The vertical markers and arrows on the tires designate the zero position and direction of positive angle measure, respectively. In these results, a total of eight SWF value ranges were established, each corresponding to an equal span of values ranging from zero to the maximum value of the particular SWF.

From Figures 6 and 7, it can be readily observed that large differences exist in the

appearance of the waveforms collected from the undamaged and damaged regions, respectively. The waveform of Figure 6 is representative of good wave transmission characteristics due to its relatively large amplitude, whereas the signal in the damaged region appears to have been almost entirely attenuated, resulting in a waveform of very small amplitude.

The quantitative analysis of the results using the stress-wave-factor method reveals that ten regions can be identified on this side of the tire as being significantly different from the remaining regions. These regions, labeled one through ten on the plot of energy for partitioned waveforms versus position on the tire shown in Figure 20, have noticeably lower SWF values from those on the rest of the tire for each SWF considered. Since all of these stress-wave-factors are related to the efficiency of energy propagation through the tire, it is reasonable to conclude that some kind of damage is present in those regions.

In order to characterize the damage apparent in the above results, X-radiographs of the tire were taken. Examination of the X-ray results indicates that eight of the ten regions identified as having significantly lower SWF values contained cord damage of varying degrees. A plot of the energy SWF for partitioned waveforms versus position on the tire is shown in Figure 21. Also included in the plot is a curve designating the regions where defects were found with X-rays. Negative values on this curve indicate areas where damaged cords were found, and positive values indicate areas where no damage was observed using X-rays. As can be seen from this plot, the SWF results correspond well with the actual damage detected with X-rays. Please notice that X-rays only detect broken cords.

An image of the X-ray corresponding to region three is shown in Figure 22. Approximately twenty four cords are damaged in this region, several of which appear completely severed while the rest are partially broken. Similar types of defects were found in regions one, four, six, seven, eight, and ten. Damage in region five corresponds to two areas where two cords in each area were slightly frayed. The nature of damage in regions two and nine is not clear at this time as X-ray results indicated no apparent cord damage in these areas. However, it can be speculated that these regions contain delaminations between the rubber and the steel cords or similar anomalies which cause large signal attenuation.

CONCLUDING REMARKS AND RECOMMENDATIONS FOR FUTURE WORK

A working prototype instrument has been developed to detect cord fatigue damage in steel-belted radial truck tires that can lead to tire failure in the "zipper" mode of failure. This "zipper detector" can detect fatigue cord damage in new or used tires and provide color-coded scans that are easily interpreted. Furthermore, this instrument is production oriented and capable of being used for on-line inspection of new or retreaded tires. However, further research and development work still remains to be carried out in several areas of this project.

Additional research and development of roller ultrasonic contact transducers is needed. Because roller ultrasonic contact transducers are currently being used, the mechanical performance of the transducer fixture should be further investigated, in particular the effects of transducer alignment and contact pressure variations on the stress-wave-factor results.

Further work should also be carried out in the area of defect characterization and calibration method to investigate the smallest defect this instrument can detect. The reliability of the test method should also be investigated through further testing.

To avoid the problems inherent with roller contact transducers, research work is also recommended in the area of remote sensors to generate and receive ultrasonic stress waves. One potential combination is to generate the ultrasonic waves using a laser and receiving the ultrasonic waves using air-coupled transducers. The main advantage of such a transmitter/receiver transducer system is the elimination of contact between the transducers and the tire surface.

ACKNOWLEDGMENTS

The authors are grateful to Dr. Robert R. Reeber from the Materials Science Division of the US Army Research Office for his support. This work was partially supported by US Army Contract DAAH04-95-1-0012.

REFERENCES

1. Anon., Annual Report, Goodyear Tire and Rubber Company, Akron, Ohio, 1989.

2. Reis, H.L.M. dos, and Warmann, K.A., "Nondestructive Evaluation of Damage in Steel Belted Radial Truck Tires," Technical Report GE91-03, Department of General Engineering, University of Illinois at Urbana-Champaign, May 1991.

3. Reis, H. L. M. dos, and Warmann, K.A., "Nondestructive Evaluation of Damage in Steel Belted Radial Tires using Acousto-Ultrasonics," *Journal of Acoustic Emission,* Vol. 11, No. 3, (1993), pp. 107-115.

4. Reis, H. L. M. dos, and Warmann, K.A., "Acousto-Ultrasonic Nondestructive Evaluation of Fatigue Damage in Steel Belted Radial Tires," INSIGHT -- *Non-Destructive Testing and Condition Monitoring,"* Vol. 36, No. 12, (1994), pp. 958-963.

5. Reis, H. L. M. dos, Warmann, K.A., "Acousto-Ultrasonic Damage Evaluation in Steel-Belted Radial Tires," Proceedings of the *Seventh International Symposium on Nondestructive Characterization of Materials*, Czech Technical University, Prague, Czech Republic, June 19-23, 1995, (8 pages).

6. Reis, H. L. M. dos, et al, "Nondestructive Evaluation of Ceramics Using the Acousto-Ultrasonic Approach and Acoustic Microscopy" Technical Report UILU ENG 90-3026, The University of Illinois at Urbana-Champaign, Urbana, Illinois, 1990.

7. "Waveform Measurements and Analysis Programs--WAVEMAP," Department of General Engineering, University of Illinois at Urbana-Champaign, Urbana, Illinois, 1989.

8. Vary, A., and Lark, F. R., "Correlation of Fiber Tensile Strength and the Ultrasonic Stress Wave Factor," NASA Lewis Research Center, Cleveland, Ohio, NASA TM 78846, 1978.

9. Williams, J. H., Jr., and Lampert, N. R., "Ultrasonic Evaluation of Impact-Damaged Graphite Fiber Composite," *Materials Evaluation*, 1980, pp. 68-72.

10. Kautz, H. E., "Ultrasonic Evaluation of Mechanical Properties of Thick, Multilayered, Filament Wound Composites," NASA Lewis Research Center, Cleveland, Ohio, NASA TM 87088, 1985.

11. Govada, A. K., Duke, J. C., Jr., Henneke II, E. G., and Stinchcomb, W., W., "A Study of the Stress Wave Factor Technique for the Characterization of Composite Materials," NASA Lewis Research Center, Cleveland, Ohio, NASA CR 174870, 1985.

12. Reis, H. L. M. dos, and McFarland, D. M., "On the Acousto-Ultrasonic Non-Destructive Evaluation of Wire Rope Using the Stress Wave Factor Technique," *The British Journal of Non-Destructive Testing*, Vol. 28, No. 3, May 1985, pp. 155-156.

13. Reis, H. L. M. dos, and McFarland, D. M., "On the Acousto-Ultrasonic Characterization of Wood Fiber Hardboard," *Journal of Acoustic Emission*, Vol. 5, No. 2, April-June 1986, pp. 67-70.

14. Reis, H. L. M. dos, Bergman, O. A., and Bucksbee, J. H., "Adhesive Bond Strength Quality Assurance Using the Acousto-Ultrasonic Technique," *The British Journal of Non-Destructive Testing*, Vol. 28, November 1986, pp. 357-358.

15. Reis, H. L. M. dos, "Nondestructive Evaluation of Adhesive Bond Strength in Laminated Wood Beams," *The British Journal of Non-Destructive Evaluation,* Vol. 31, No. 12, December, 1989, pp. 675-679.

16. Reis, H. L. M. dos, "Acousto-Ultrasonic Assessment of Finger Joint Integrity in Structural Lumber," *British Journal of Non-Destructive Testing, Vol.* 32, No. 10, 1990, pp. 509-510.

17. "Analytical Ultrasonics in Materials Research and Testing," NASA Conference Publication 2383, V. Vary, Editor, NASA Lewis Research Center, Cleveland, Ohio, November 13-14, 1984.

18. "Acousto-Ultrasonics--Theory and Application, " J. C. Duke, Jr., Ed., Plenum Press, New York, N. Y., 1989.

19. "Nondestructive Testing and Evaluation for Manufacturing and Construction, " H. L. M. dos Reis, Ed., Hemisphere Publishing Corporation, New York, N. Y., 1990.

Figure 1 (a) Overall photograph of machine with tire

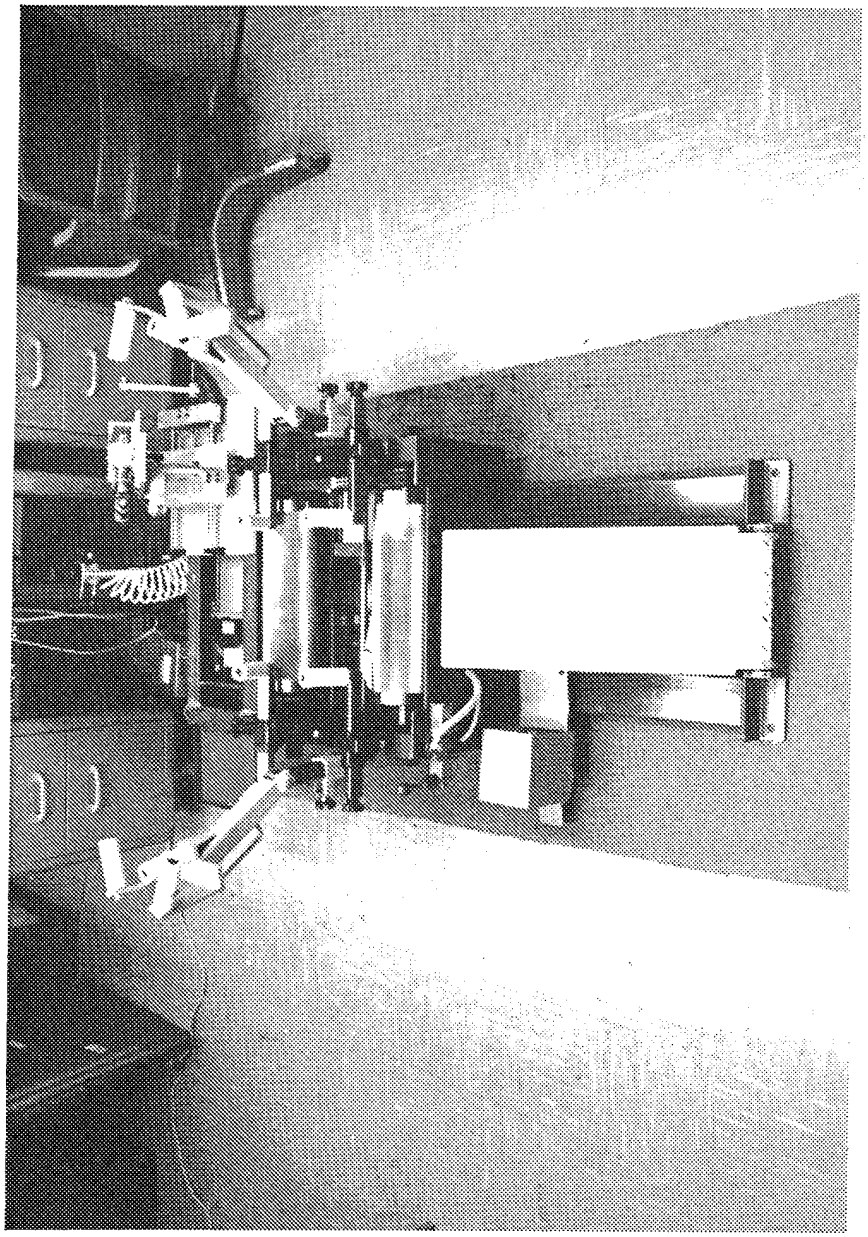

Figure 1 (b) Close-up photograph of machine

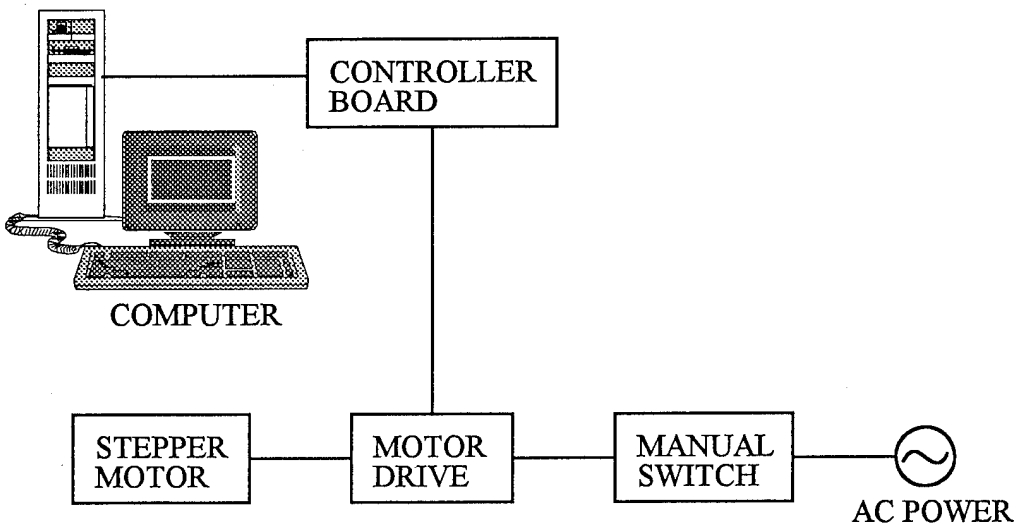

Figure 2 Schematic of motor control system

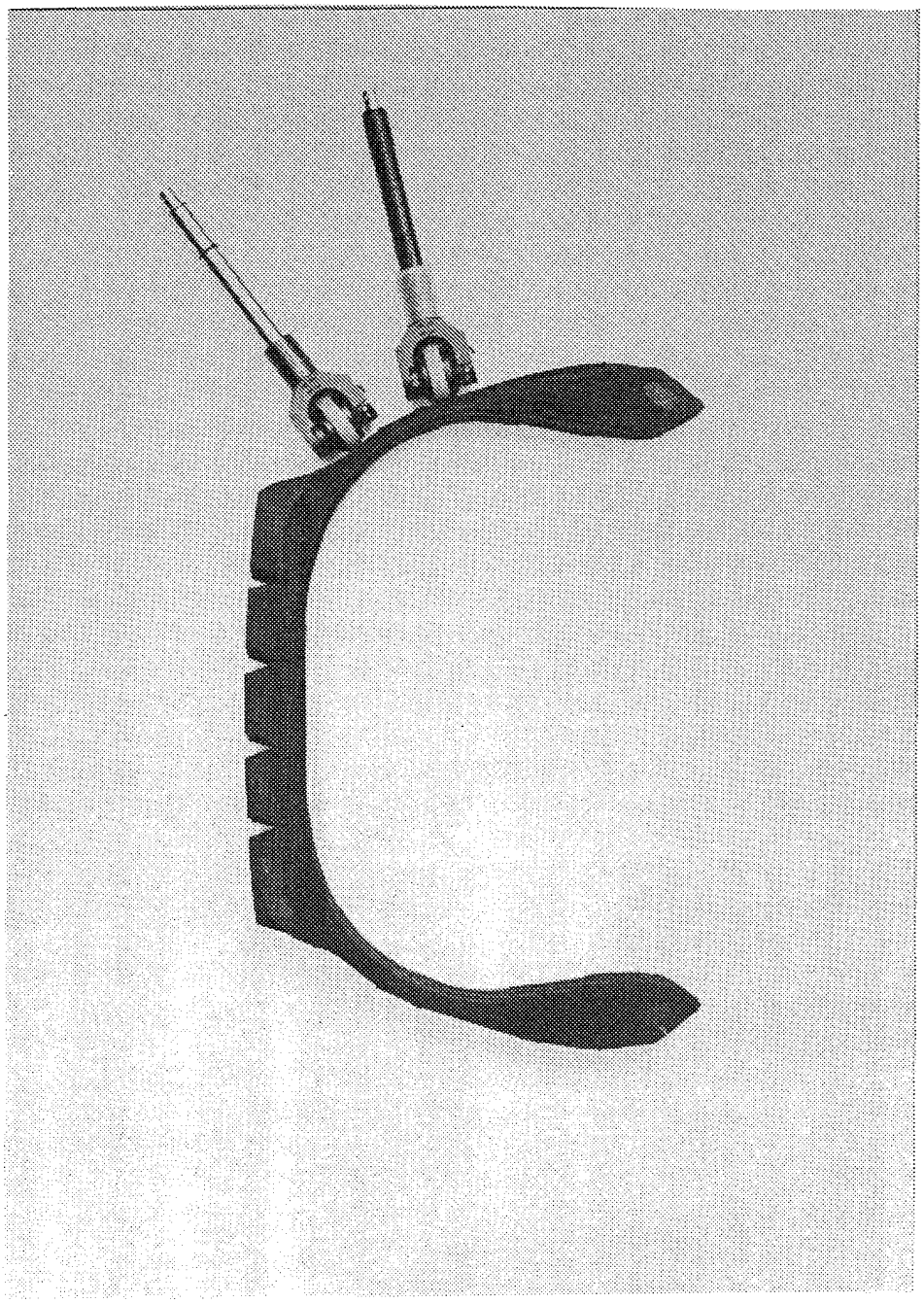

Figure 3 Photograph of ultrasonic roller transducers with cross section of a tire

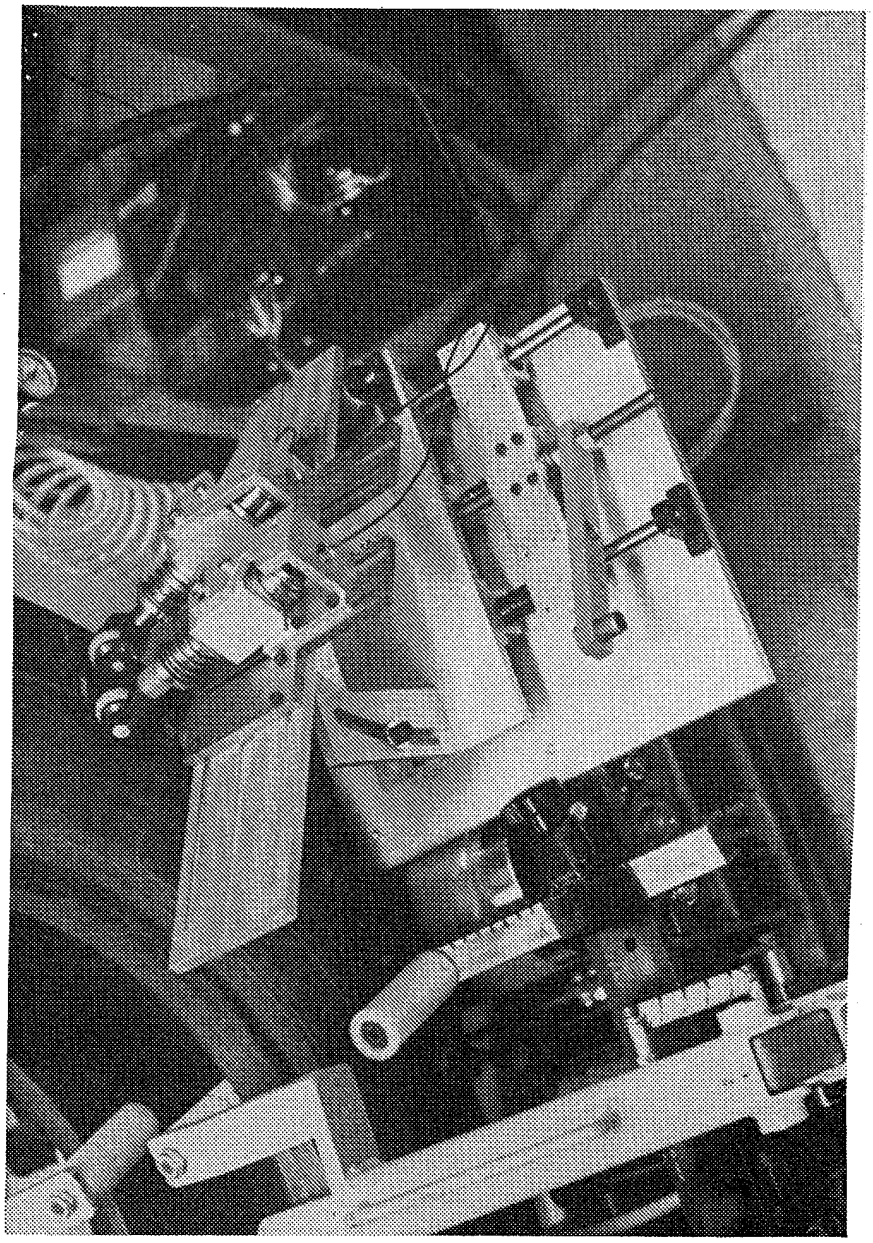

Figure 4 Photograph of fixture mounted on the machine

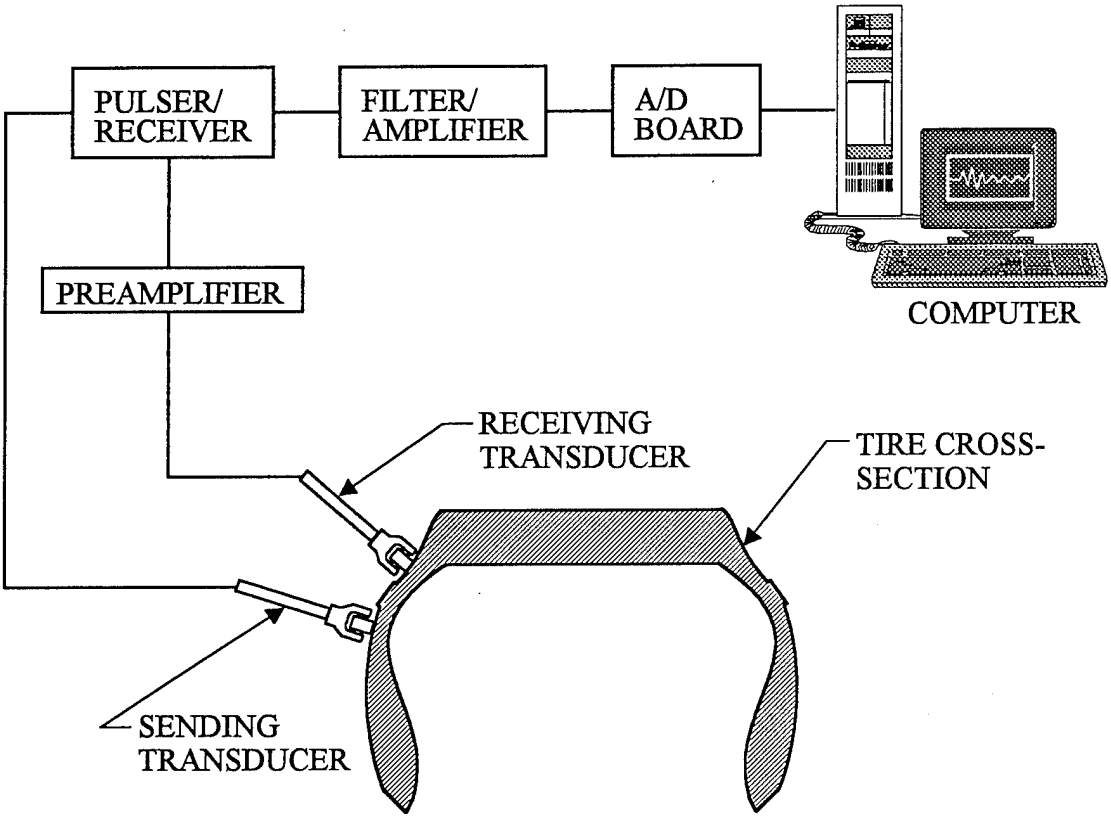

Figure 5 Schematic of data acquisition system

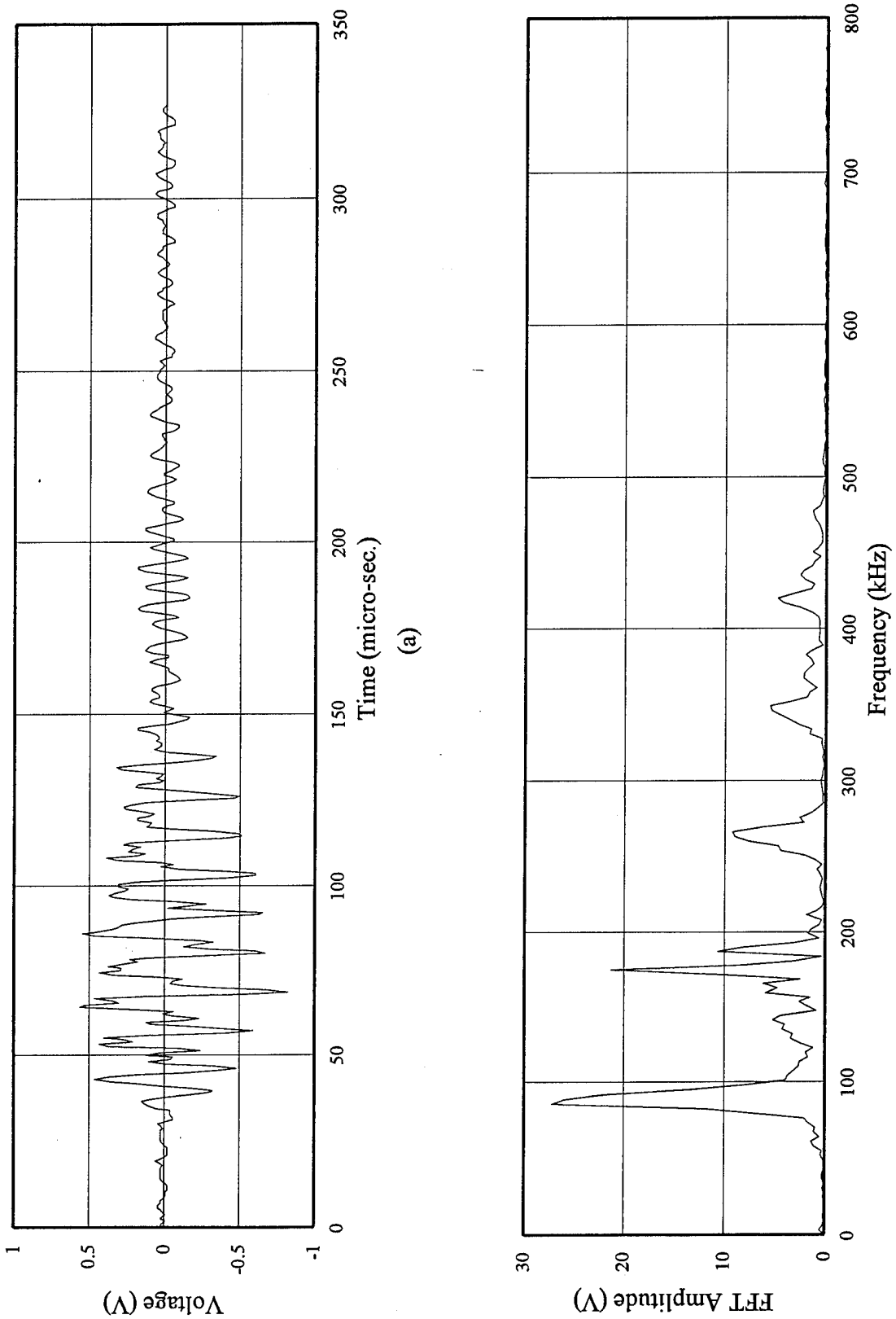

Figure 6 Typical waveform (a) and frequency spectrum (b) obtained from an undamaged region in the tire

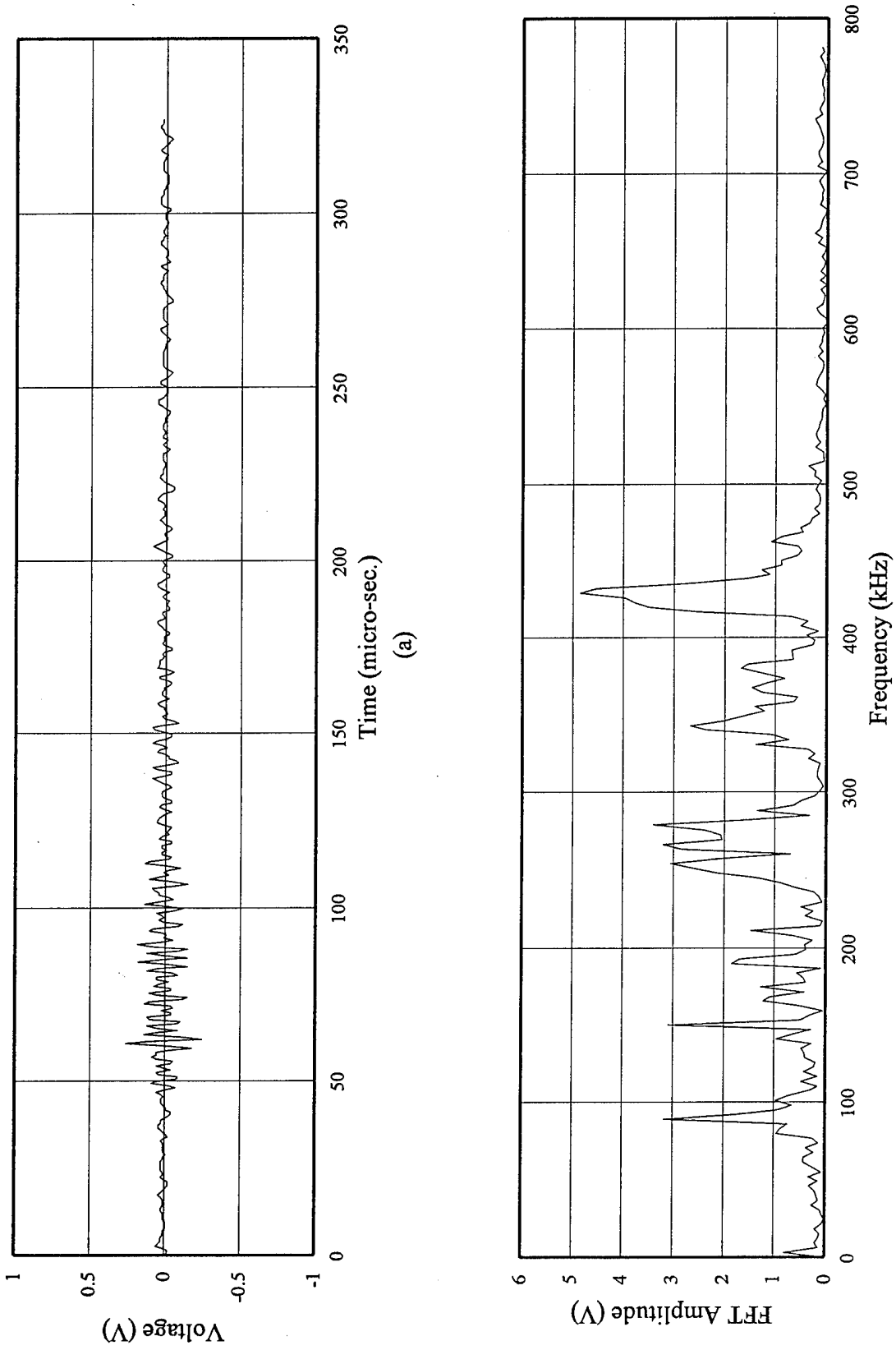

Figure 7 Typical waveform (a) and frequency spectrum (b) obtained from a damaged region in the tire

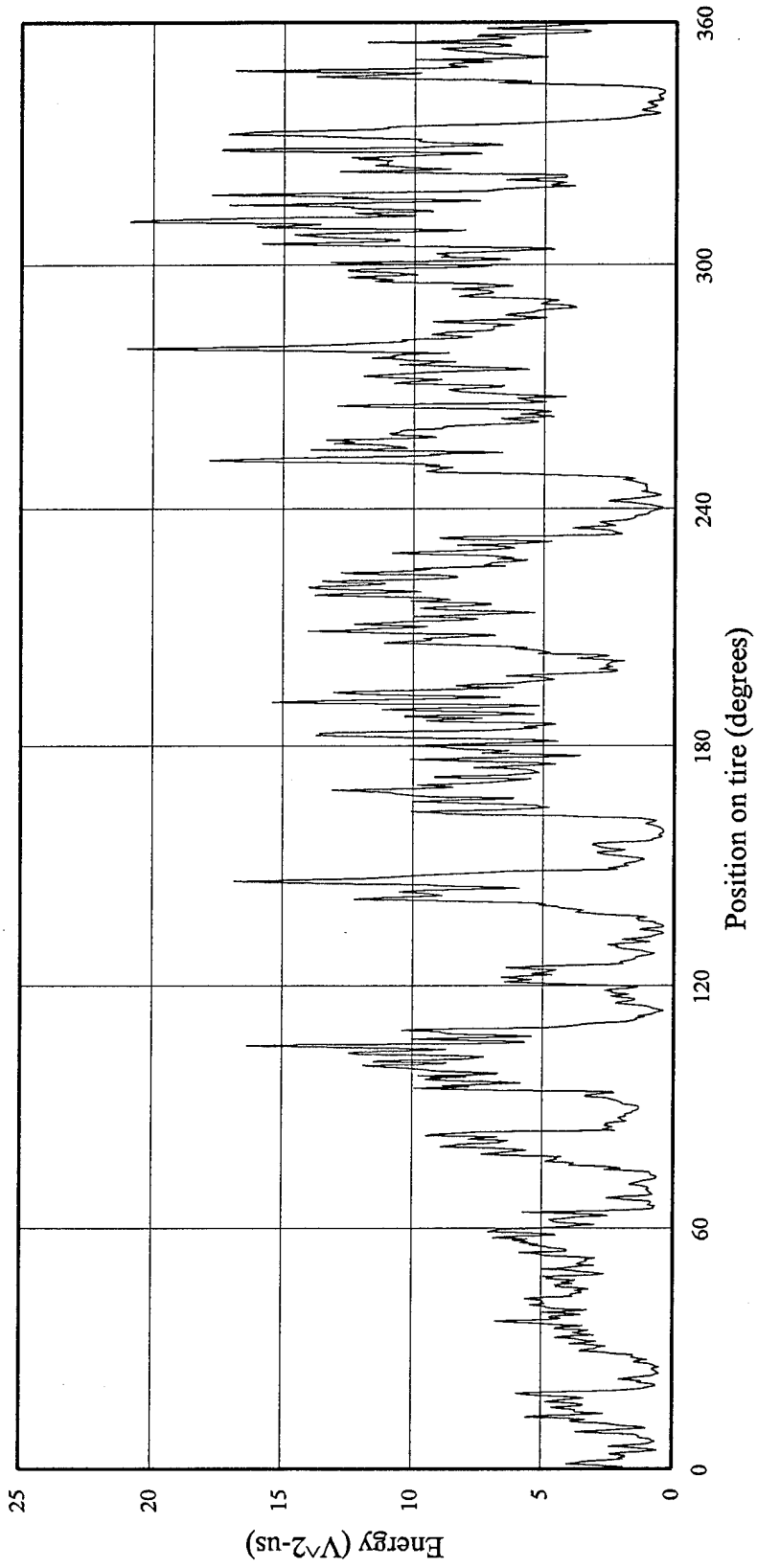

Figure 8 Plot of energy versus position on tire for entire waveforms

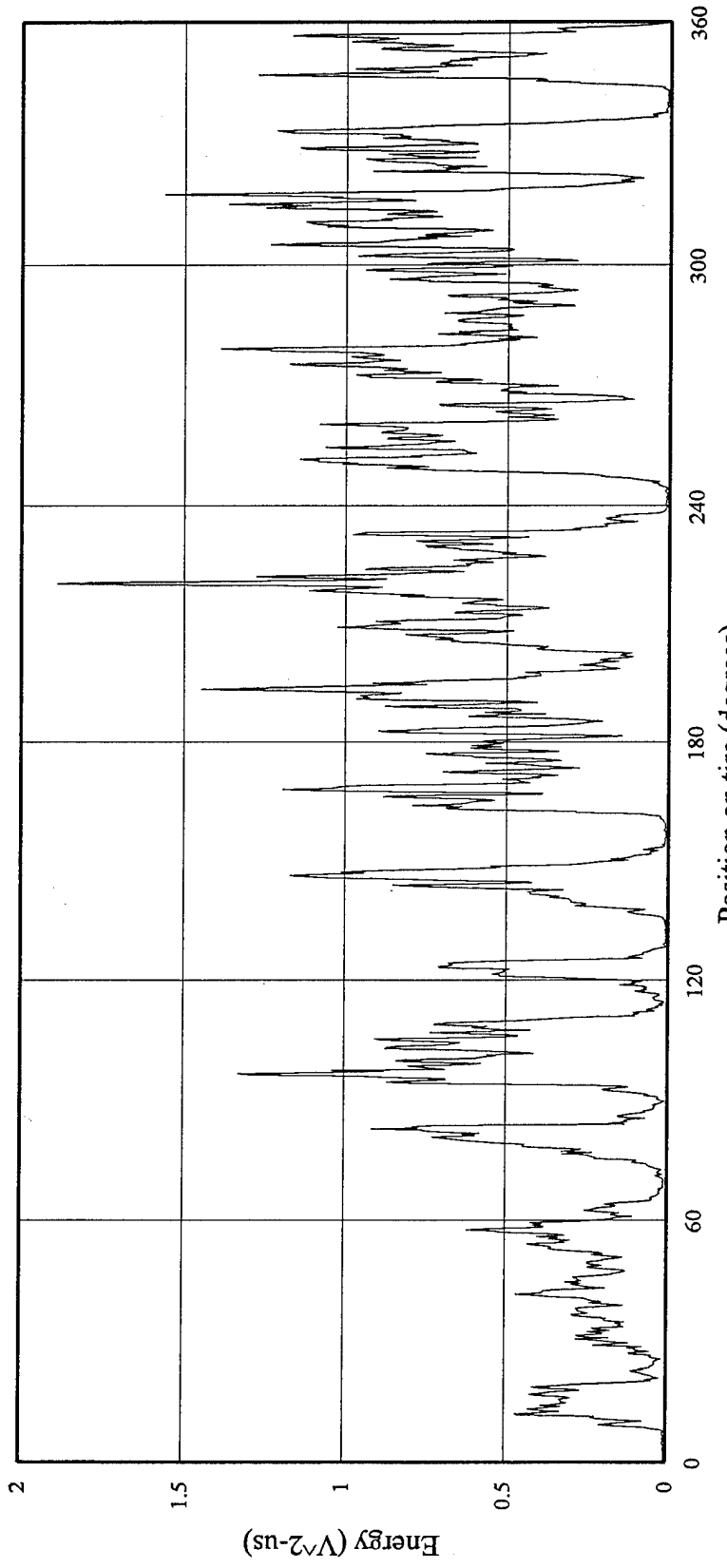

Figure 9 Plot of energy versus position on tire for a 26.9 - 45.4 micro-second partition of waveforms

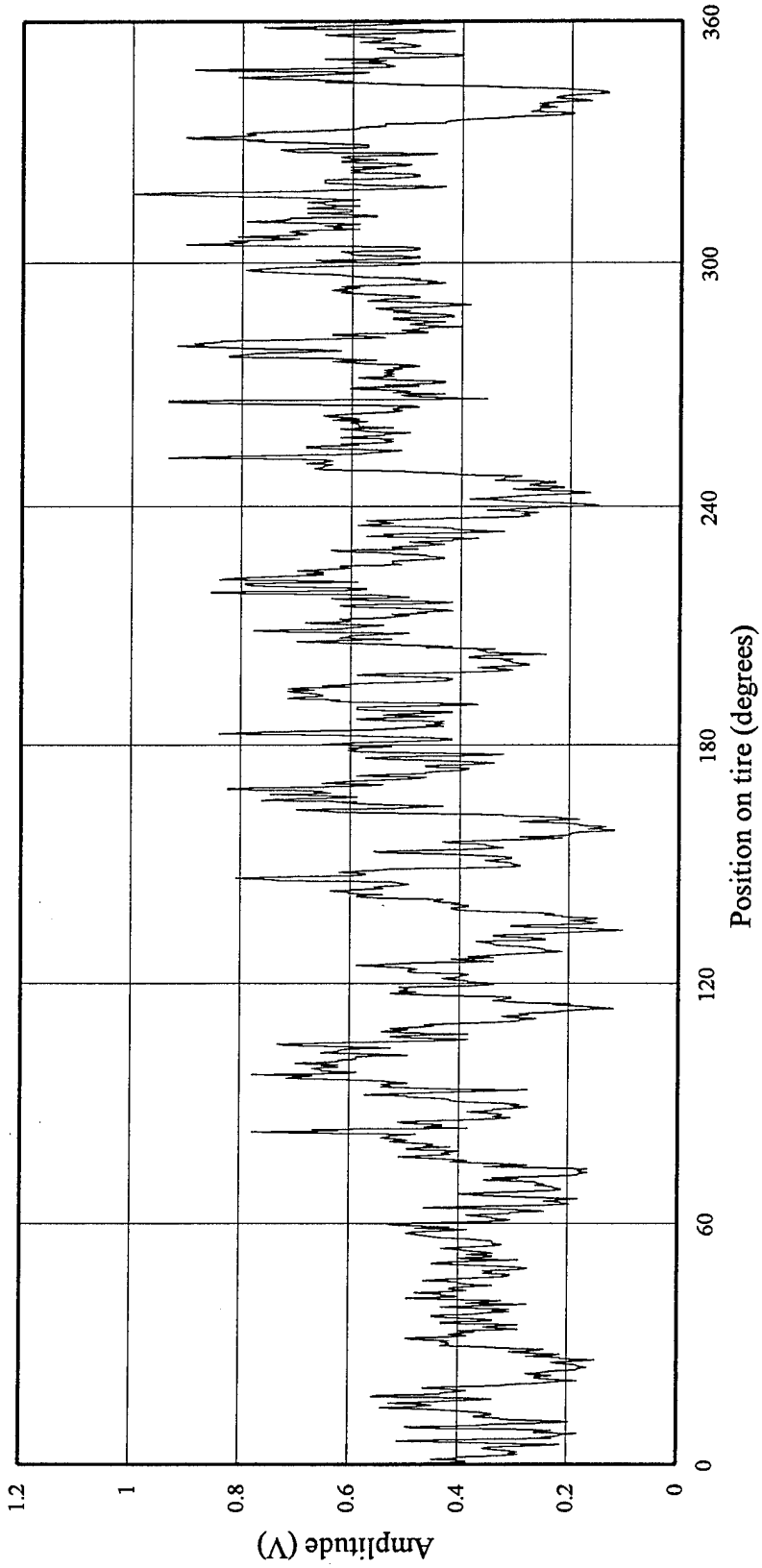

Figure 10 Plot of peak amplitude in time domain versus position on tire for entire waveforms

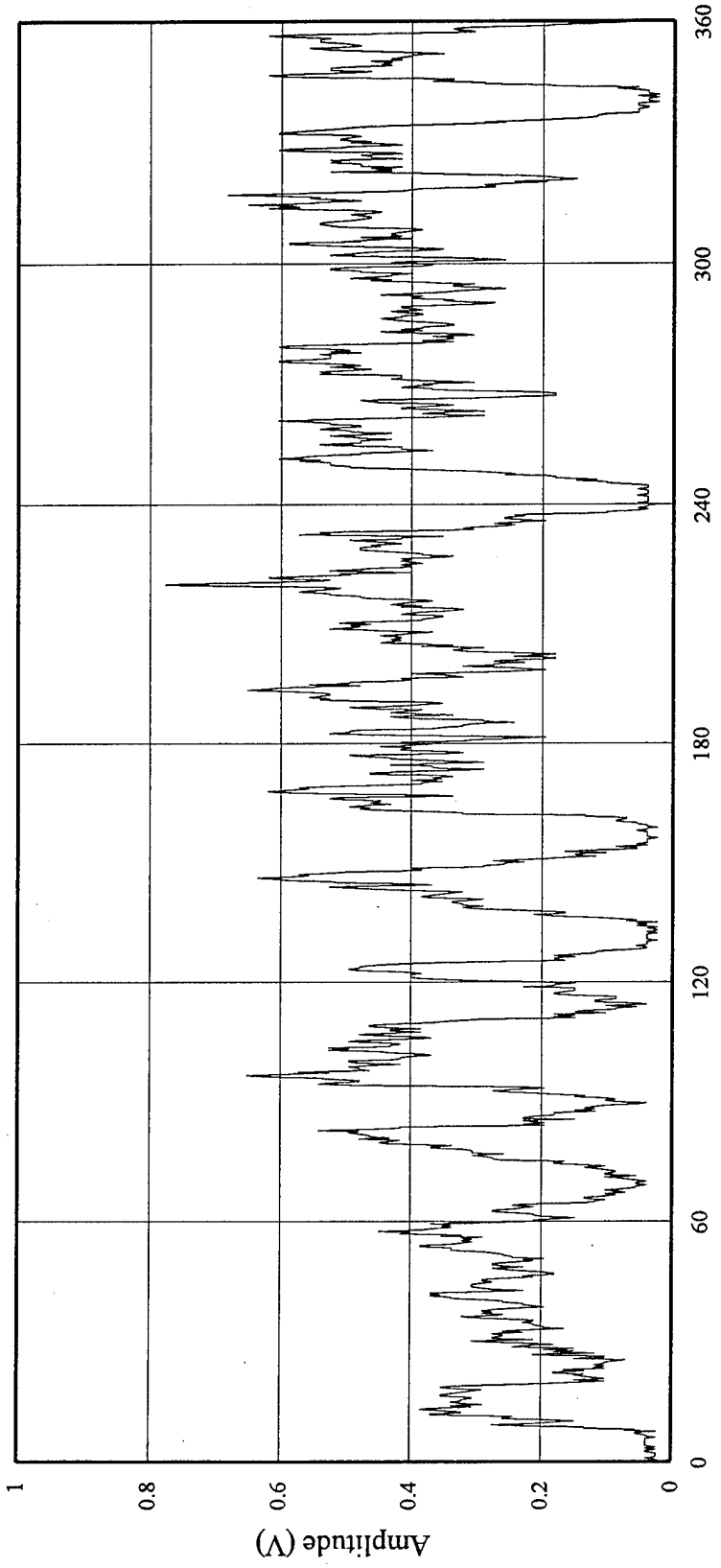

Figure 11 Plot of peak amplitude in time domain versus position on tire for 26.9 - 45.4 micro-second partition of waveforms

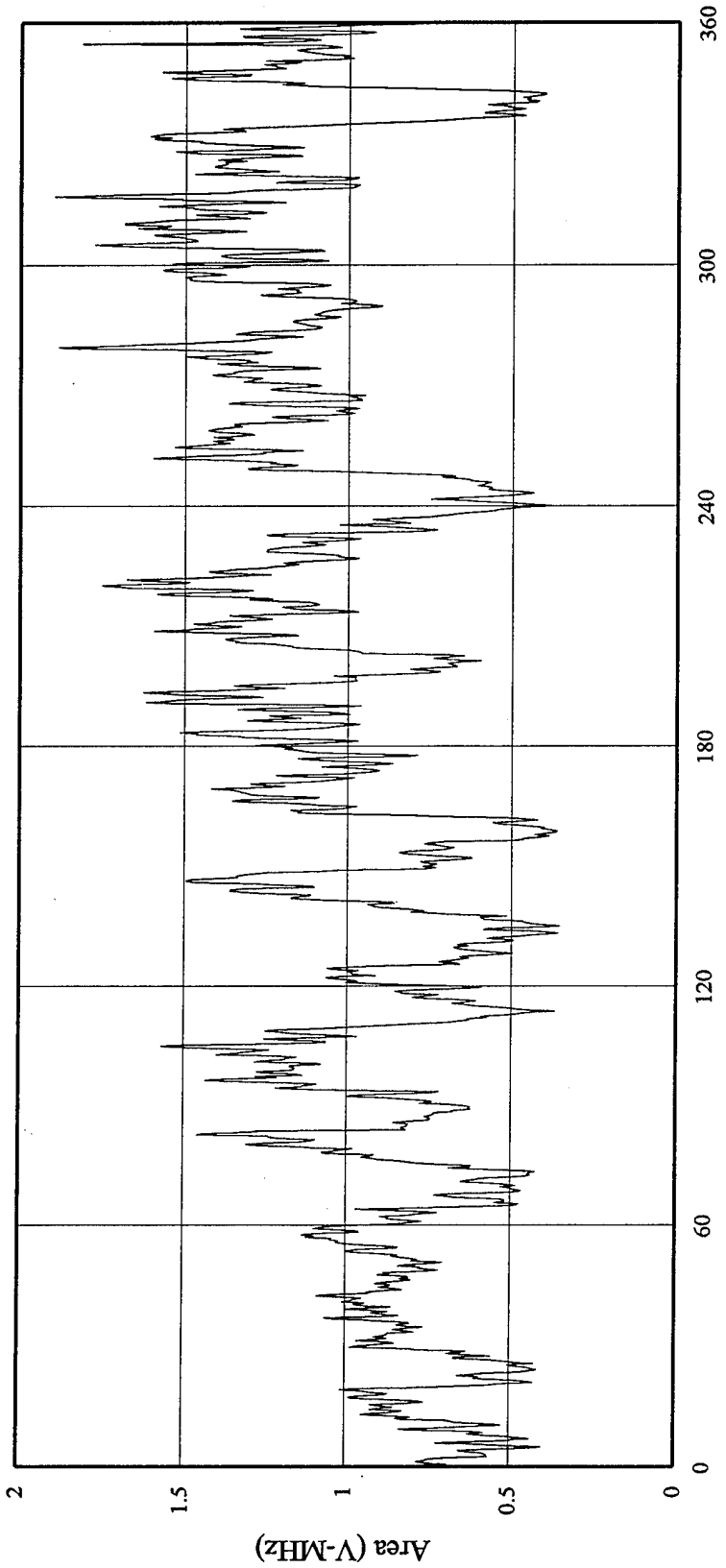

Figure 12 Plot of area under the power spectral density curve in the frequency domain versus position on tire for entire waveforms

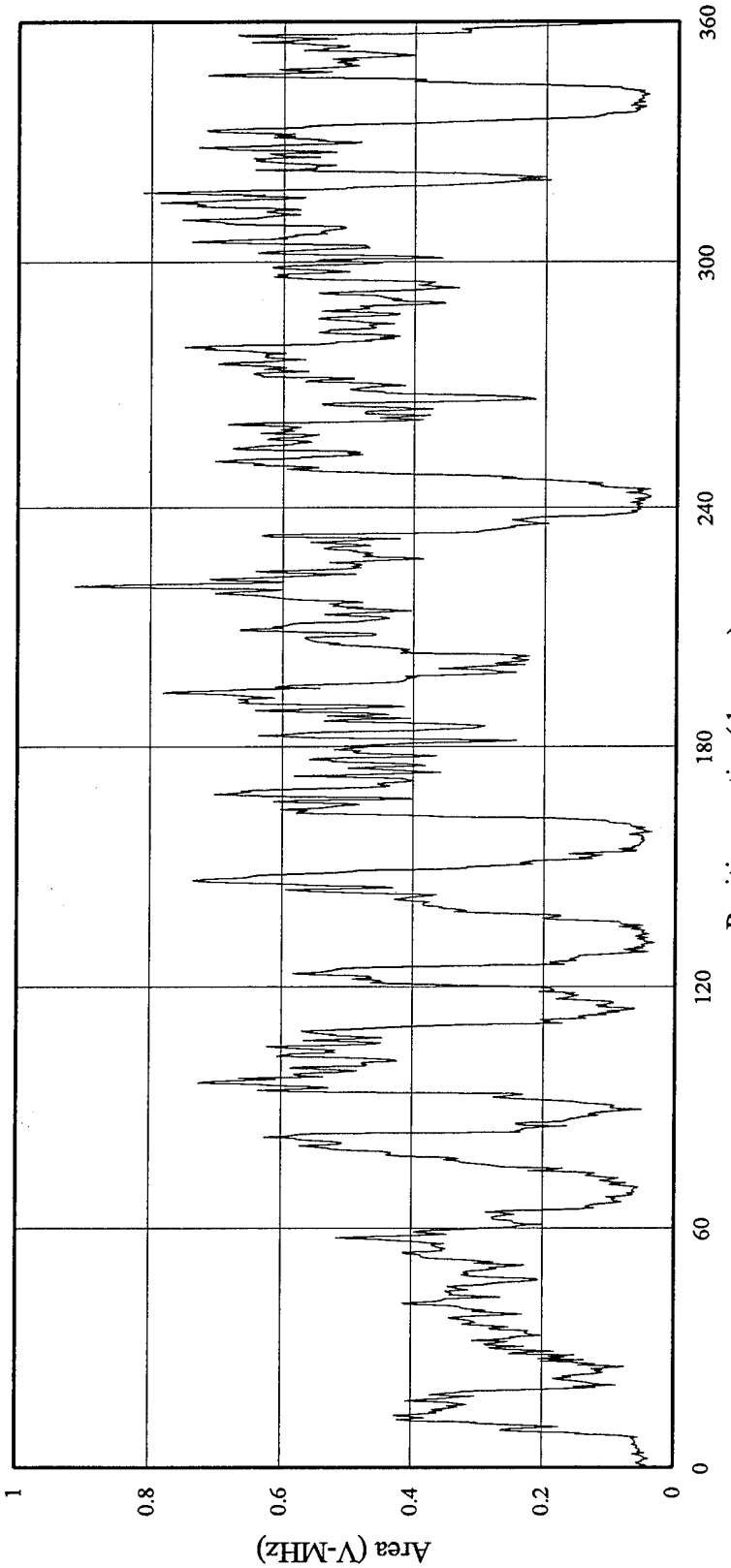

Figure 13 Plot of area under the power spectral density curve in the frequency domain versus position on tire for 26.9 - 45.4 micro-second partition of waveforms

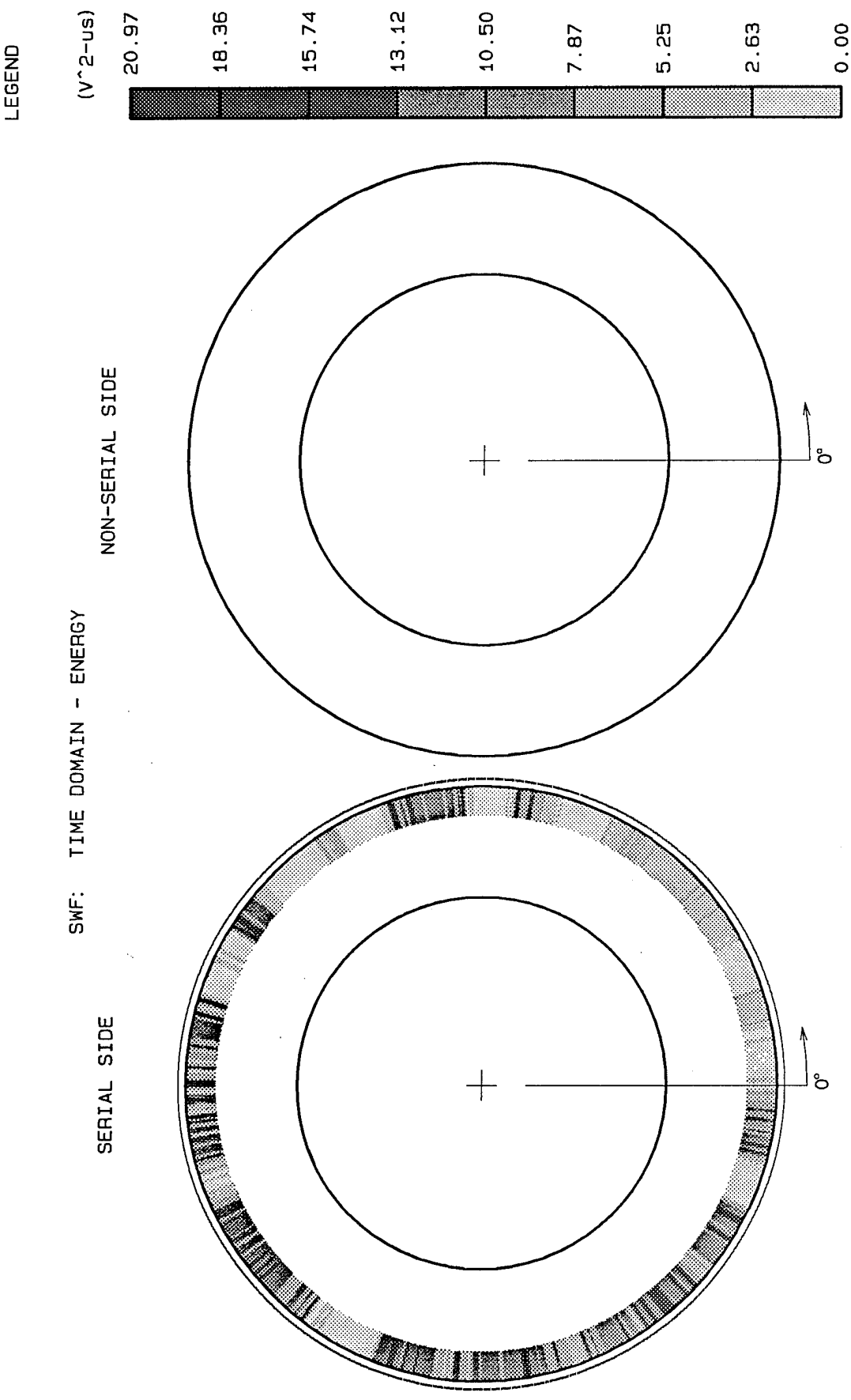

Figure 14 Two dimensional tire representation of the energy SWF for entire waveforms

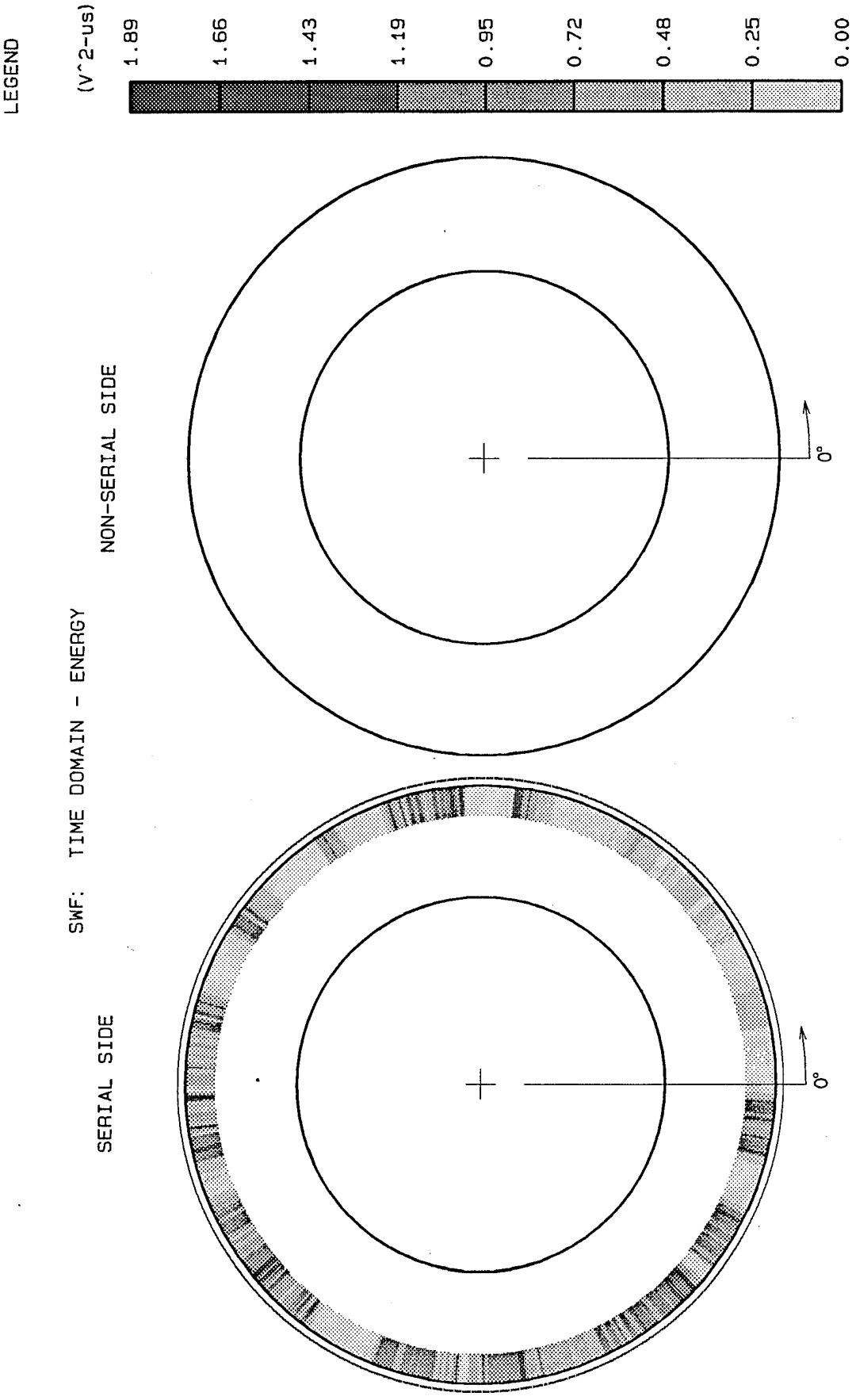

Figure 15 Two dimensional tire representation of the energy SWF for 26.9 - 45.4 micro-second partition of waveforms

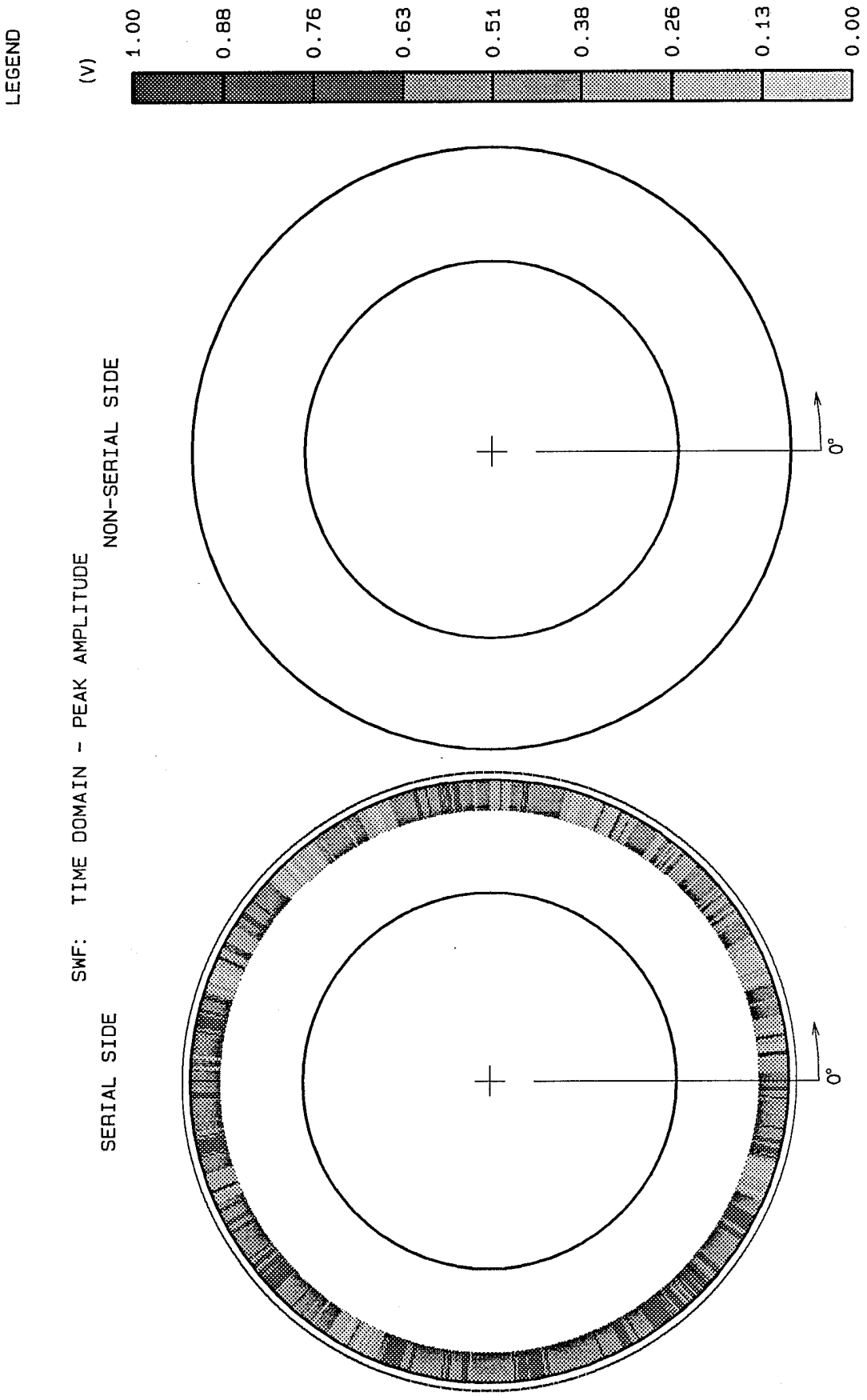

Figure 16 Two dimensional tire representation of the peak amplitude in the time domain SWF for entire waveforms

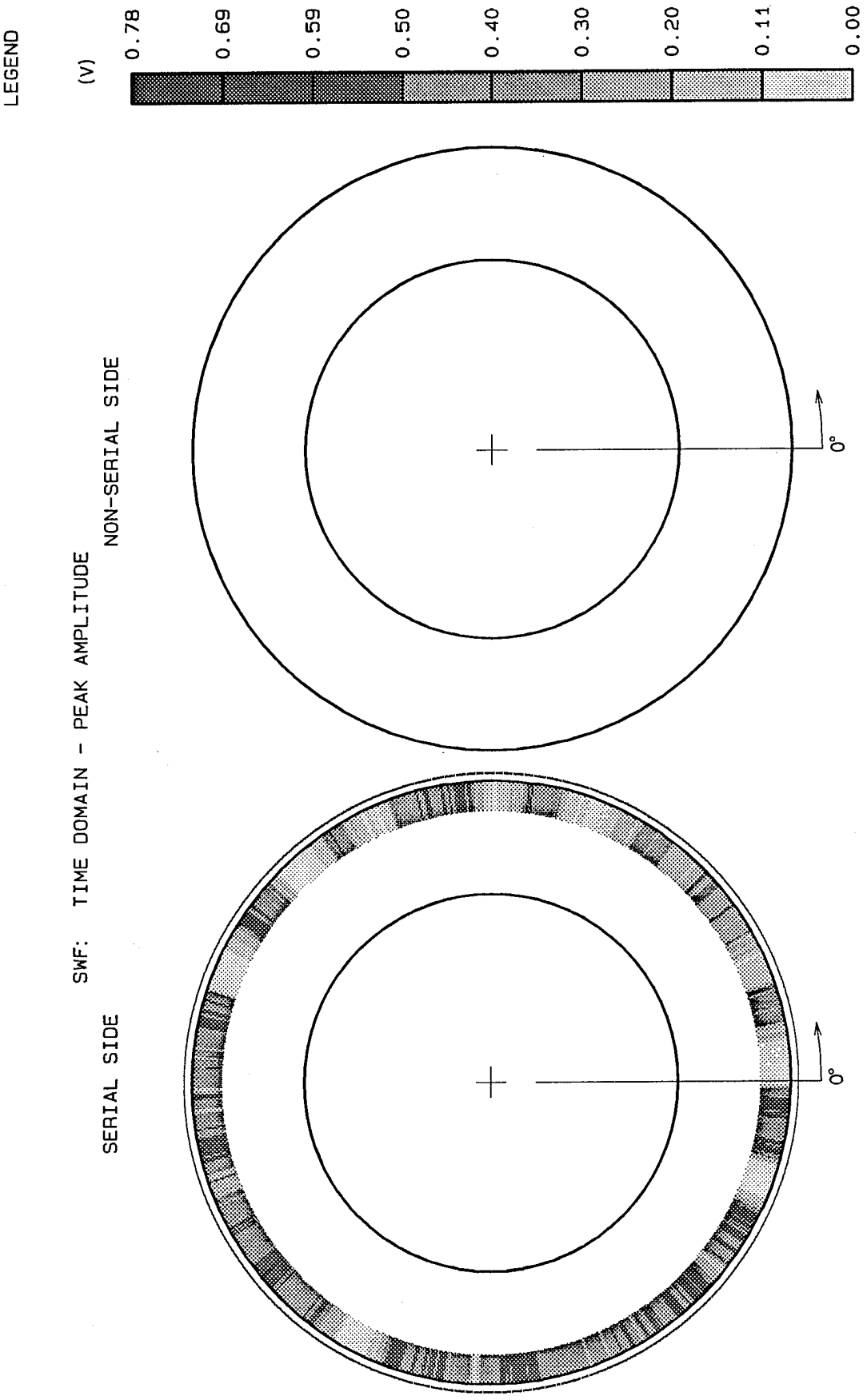

Figure 17 Two dimensional tire representation of the peak amplitude in the time domain SWF for 26.9 - 45.4 micro-second partition of waveforms

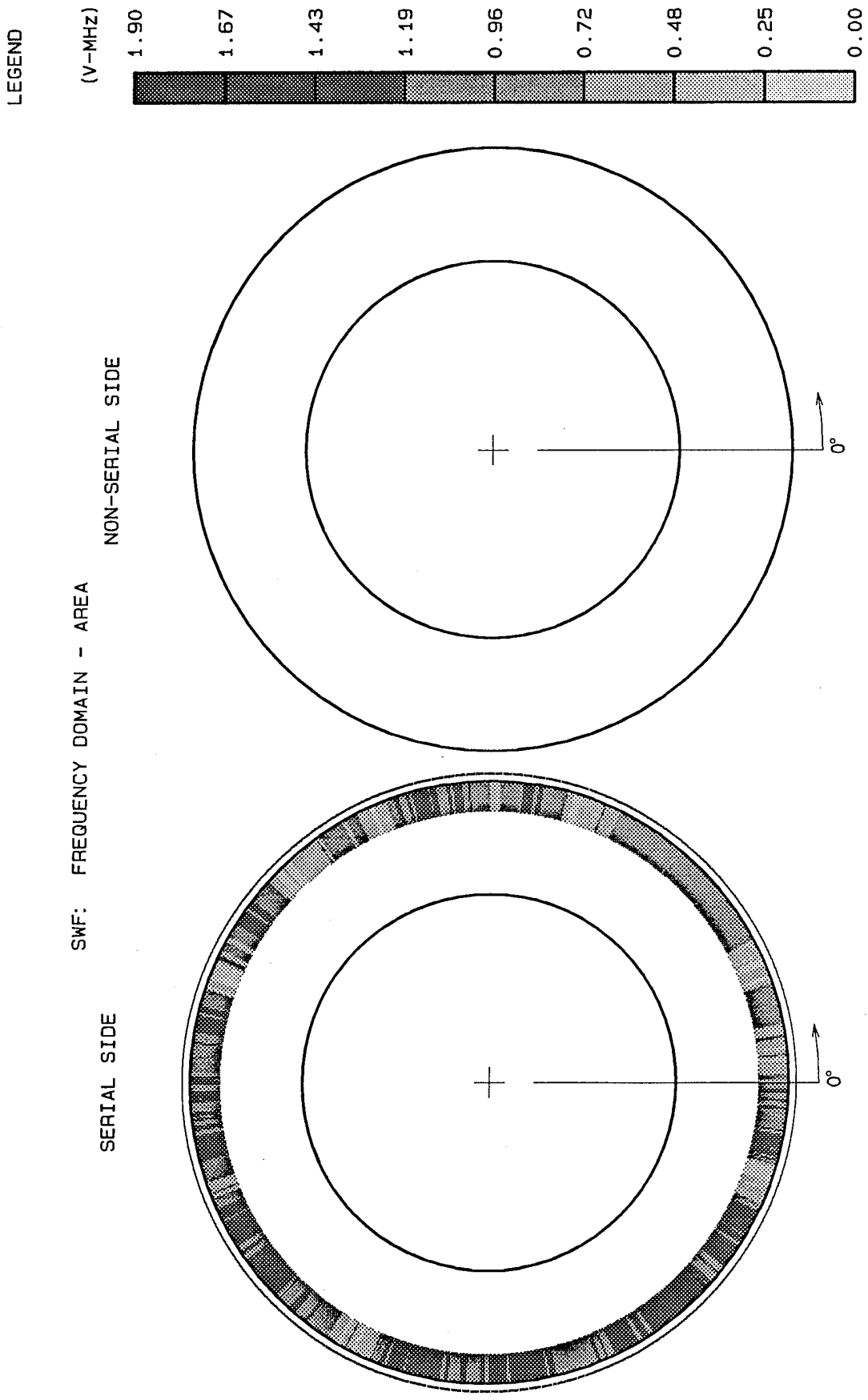

Figure 18 Two dimensional tire representation of the area under the power spectral density curve in the frequency domain SWF for entire waveforms

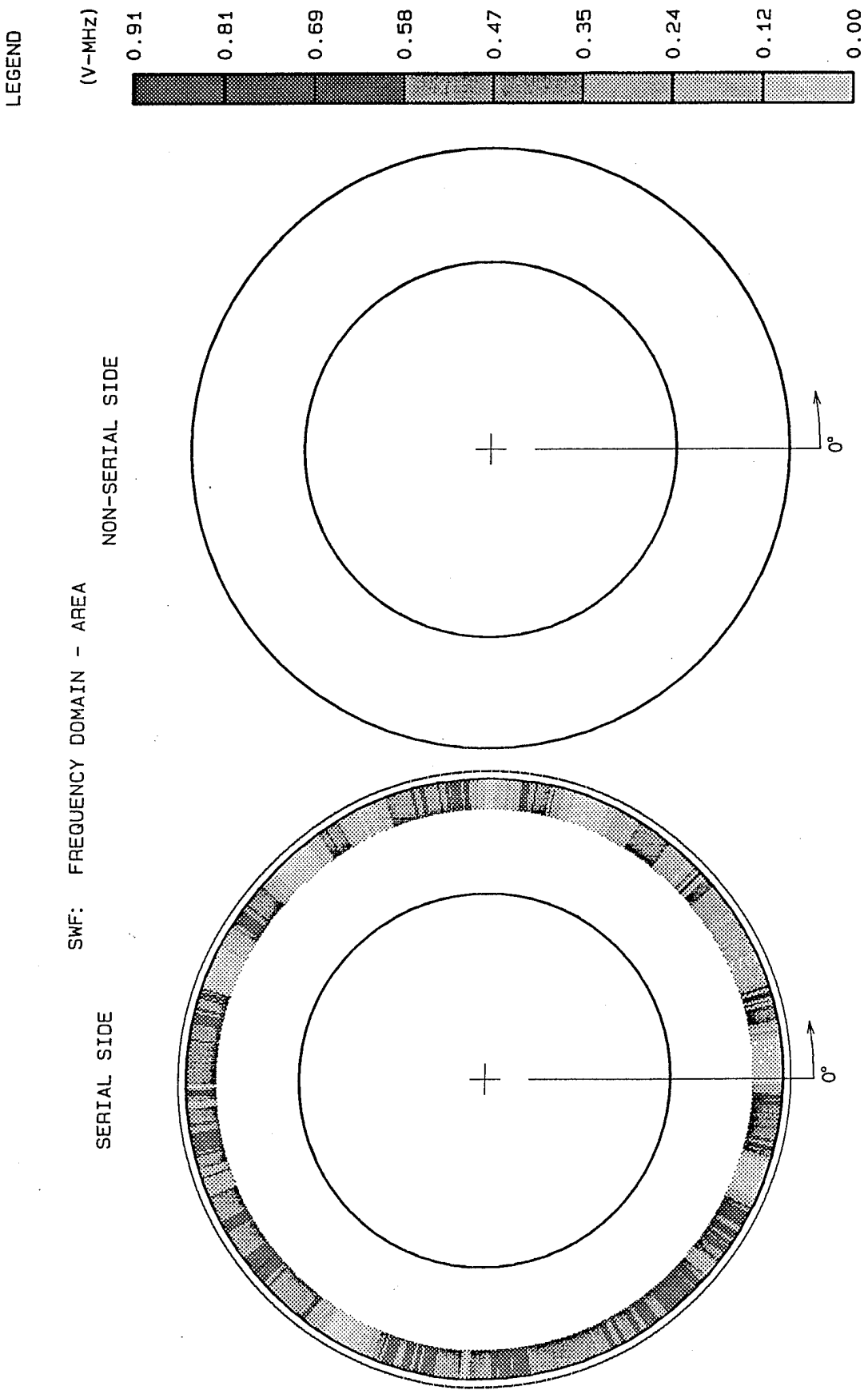

Figure 19 Two dimensional tire representation of the area under the power spectral density curve in the frequency domain SWF for 26.9 - 45.4 micro-second partition of waveforms

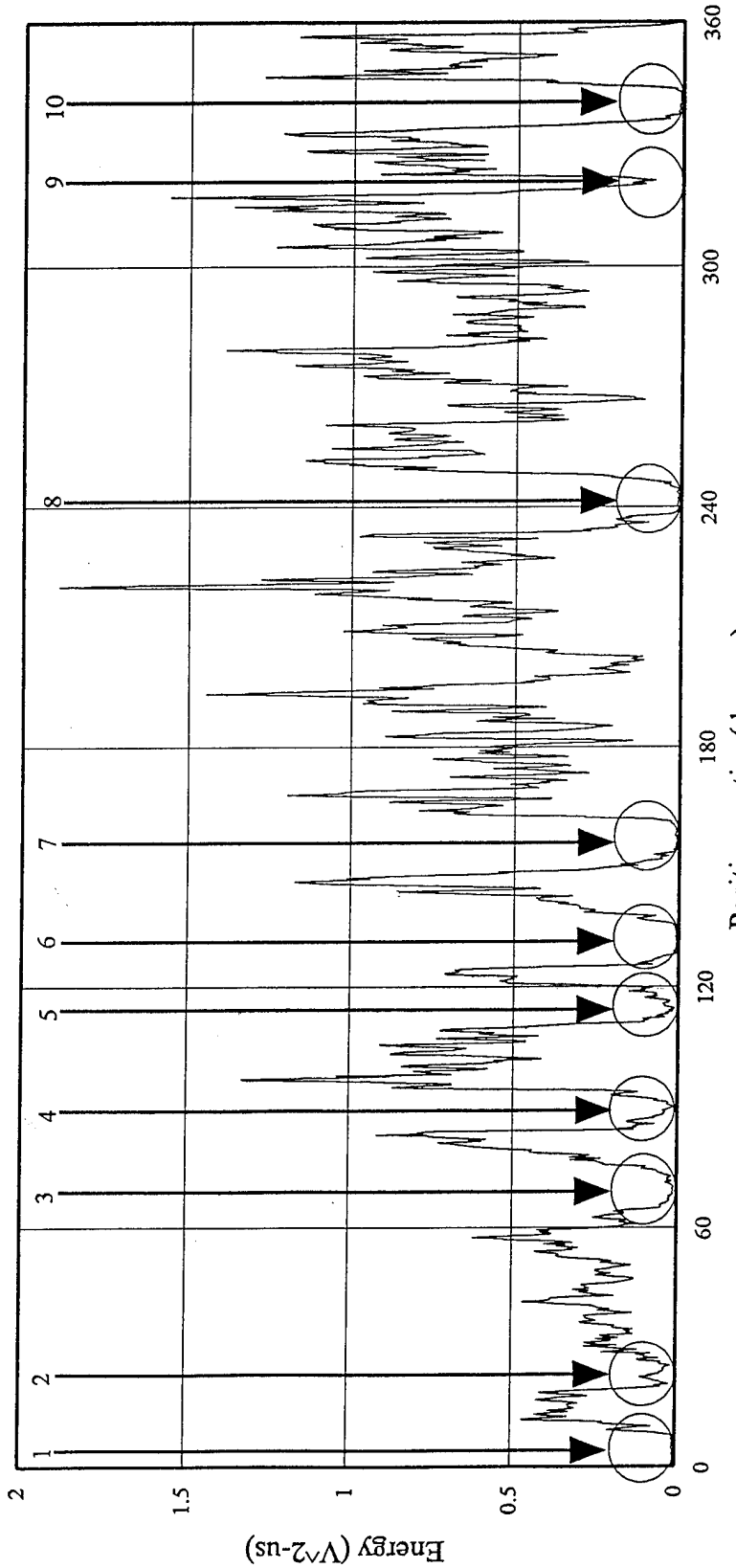

Figure 20 Plot of energy versus position on tire for a 26.9 - 45.4 micro-second partition of waveforms with ten regions suspected of containing damage

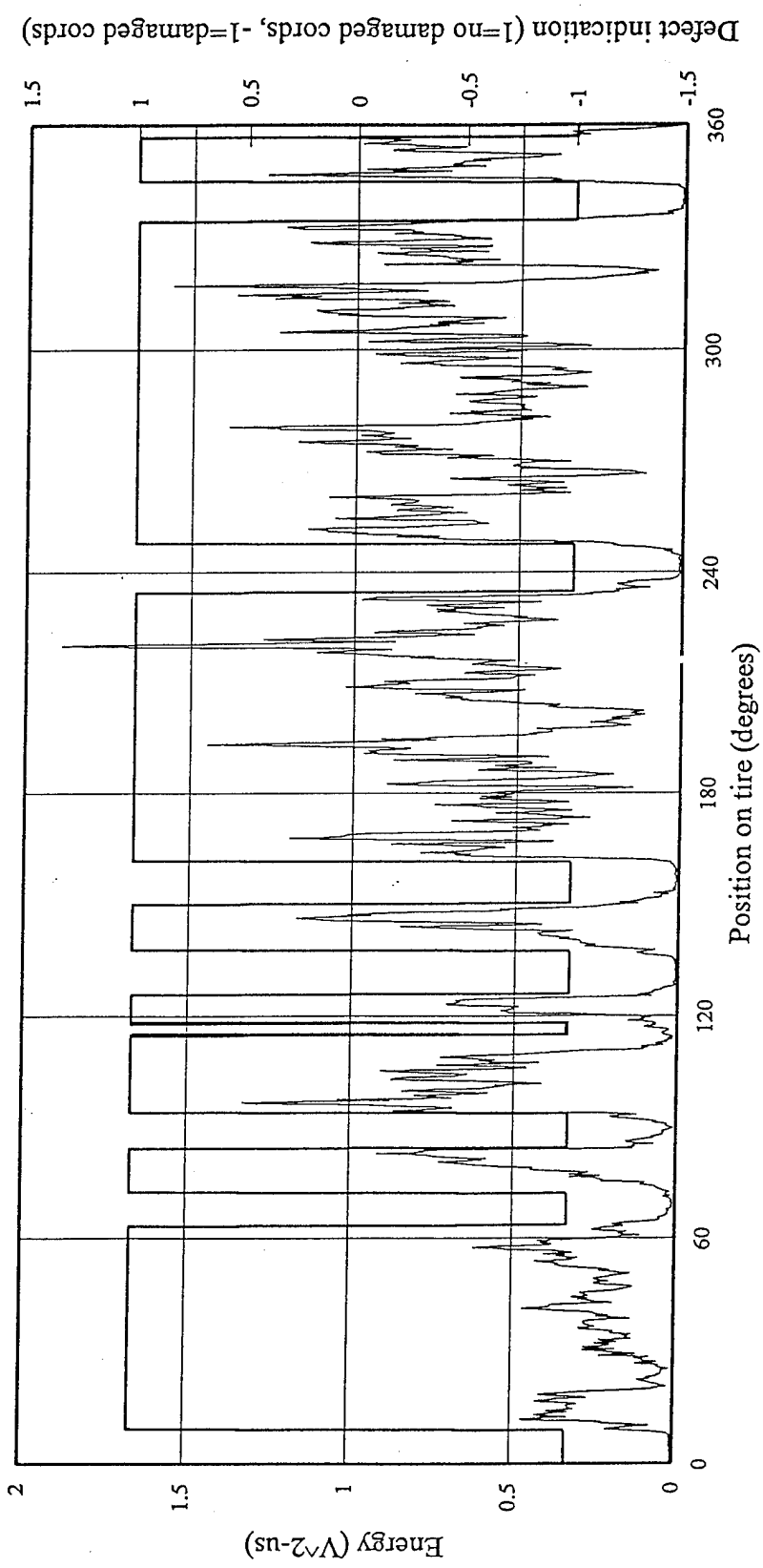

Figure 21 Plot of energy versus position on tire for a 26.9 - 45.4 micro-second partition of waveforms with curve indicating cord damage observed from X-ray examination.

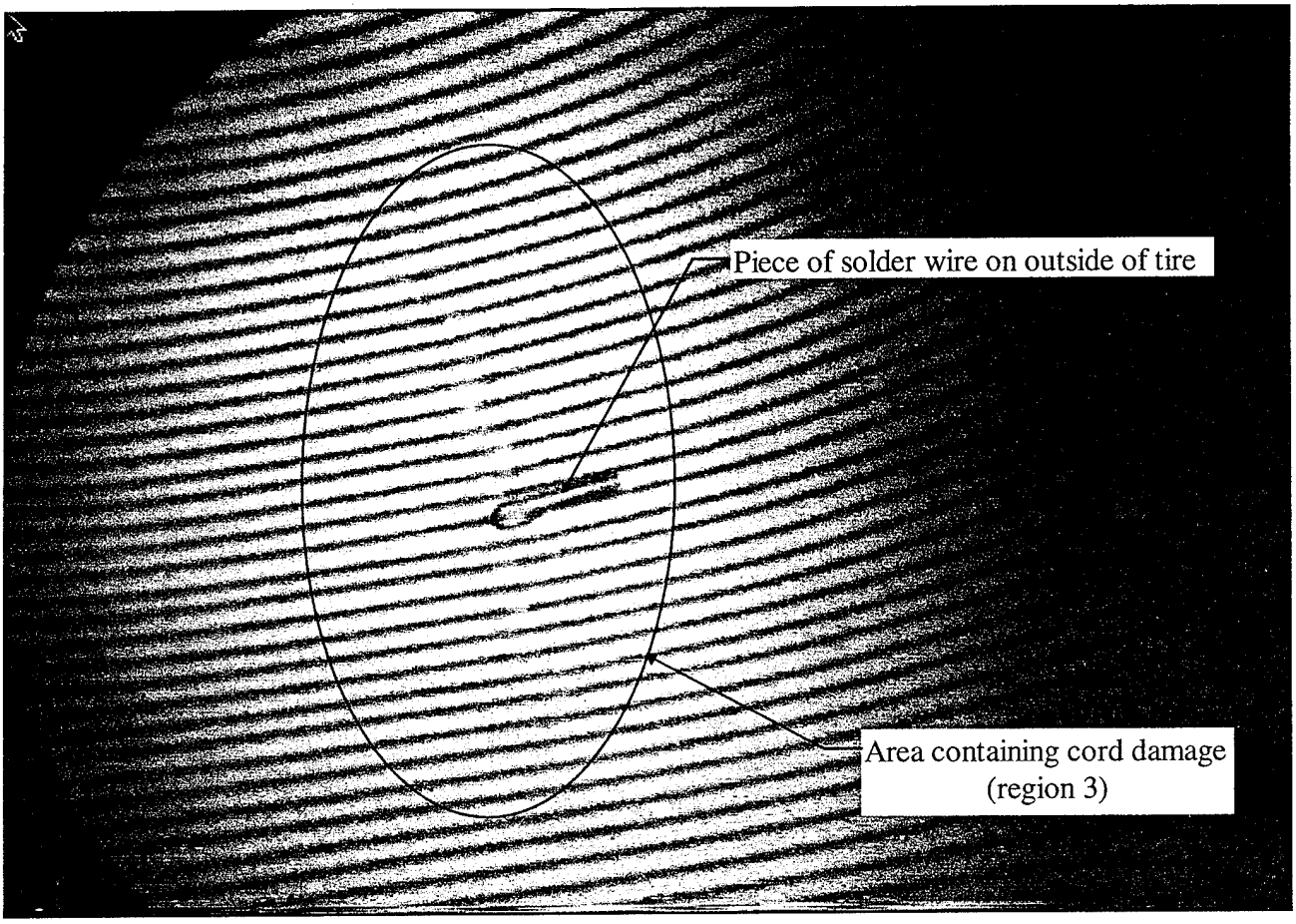

Figure 22 X-ray image of region three